ELSEVIER

Journal of Hazardous Materials B91 (2002) 187–203

Journal of Hazardous Materials

www.elsevier.com/locate/jhazmat

Adsorption of zinc by activated carbons prepared from solvent extracted olive pulp

Polymnia Galiatsatou [a,*], Michail Metaxas [a], Vasilia Kasselouri-Rigopoulou [b]

[a] *Institute of Technology of Agricultural Products, Nagref, 1 S. Venizelou, 141 23 Lykovrissi, Greece*
[b] *Department of Chemical Engineering, National Technical University of Athens, 9 Iroon Polytechniou, 157 73 Athens, Greece*

Received 22 May 2001; received in revised form 12 July 2001; accepted 1 December 2001

Abstract

Activated carbons have been prepared by a two-step physical activation with steam at different burn-off levels to study the porosity development and its effect in zinc adsorption from aqueous solutions. The main material used was the residual from the extraction with solvent of the kernel-oil [solvent extracted olive pulp (SEOP)]. Olive, apricot and peach stone have been also used as different precursors. The products were characterized by N_2 at 77 K adsorption, Hg porosimetry and iodine number determination. The influence of surface complexes and pH has been investigated in an attempt to elucidate the adsorption phenomena. The effect of different treatments [demineralization with H_2SO_4 and oxidation with $(NH_4)_2S_2O_8$] was also evaluated for the adsorption of zinc species.

Both basic and acidic carbons, originated from SEOP, show remarkable adsorption ability at solution pH = 7. Their adsorption ability mainly depends on the content and nature of functional surface groups, the ash content of the precursors and the pH of the solution. These activated carbons were proved to be efficient adsorbents for the removal of water pollutants and contaminants.

Keywords: Zinc; Adsorption; Olive pulp; Activated carbon; Surface groups

1. Introduction

In the past decades, a remarkable increase of metal contaminant volume has posed many serious environmental problems. The most common treatment processes like chemical precipitation and ion exchange are usually effective in reducing the extent of contamination, but are of moderate economic interest [1]. The use of activated carbon has emerged as one of the most effective technologies for removing organic and inorganic pollutants from

* Corresponding author. Tel.: +30-10284-5940; fax: +30-10284-0740.
E-mail address: gal.itap@nagref.gr (P. Galiatsatou).

0304-3894/02/$ – see front matter
PII: S0304-3894(02)00008-0

water and wastewater [2]. The search for cost-effective adsorbents has become the focus of attention of many researchers. In the case of using activated carbon for the removal of heavy metal pollutants from large volume of waste waters and other aqueous systems, the cost difference in comparison with ion exchangers is under investigation, taking into account that the adsorption capacity of activated carbons is comparable to that of the ion-exchangers.

Activated carbons are unique adsorbents because of their extended surface area, microporous structure, high adsorption capacity and high degree of surface reactivity. Mainly, the presence or absence of different surface functional groups, especially oxygen groups, causes the phenomenon of ion adsorption on activated carbons. The equilibrium between these groups and the solution depends on the pH of the solution [2]. It has been reported that the most important phenomena that influence the ion adsorption capacity are ion exchange, non-specific sorption, surface precipitation, redox reactions and formation of surface chelates [3–7]. Contribution of the above phenomena to ion adsorption depends on specific ion properties, the kind of surface groups and their concentrations. Specific electrochemical and adsorption properties of carbons, resulting from their structure and surface chemical properties [3,6], make them attractive in some analytical operations. The presence of ash has also been reported to influence the adsorption mechanism either via ion exchange or due to the catalytic effect of inorganic matter [8].

Agricultural by-products (fruit stones, shells, seeds and olive stones) derived from the processing of fruits and olives, have been used for the preparation of activated carbons with a high adsorption capacity, considerable mechanical strength and low ash content [9–11].

Greece is the third larger producer of olive oil, in the world. Every year hundred tons of solvent extracted olive pulp (SEOP) is produced which are either rejected to the environment or used as a fuel but with low calorific value. A better way to give to this inexpensive by-product an added value is to use it as a precursor for the preparation of activated carbon.

Regeneration of the activated carbons is viable via desorption of the heavy metals, under suitable conditions, so as these adsorbents could be useful in metal ion recycling process [12,13].

The objective of this study is to investigate the capacity of carbons with basic behavior, produced from SEOP, on Zn^{2+} adsorption from aqueous solutions. The effect of the steam activation procedure for different periods of time, the treatment of the precursor with H_2SO_4 and the oxidation of activated carbon with $(NH_4)_2S_2O_8$, was investigated on Zn^{2+} adsorption. The changes in the surface chemistry upon different treatments were also studied. The adsorption ability was correlated to the surface chemistry and the ash content of the activated carbons as well as to the pH of the solution. Olive, apricot and peach stone have been also used as different precursors. Zinc was selected for the adsorption experiments due to its solubility in a wide pH range and its presence in several industrial waste waters.

2. Experimental

2.1. Sample preparation

Activated carbons from SEOP have been used in this study. Olive, peach and apricot stone were also used to prepare activated carbons for comparative purpose. The raw materials were

crushed and sieved to a particle size of 2.5–3.5 mm. Samples derived from SEOP, olive, peach and apricot stone (coded as ACOP, ACO, ACP and ACA, respectively) were prepared by carbonization in N_2 at 1123 K for 1 h 30 min with a heating rate of 10 °C/min. Activation was applied by means of a steam/nitrogen mixture (flow rate 100 ml/min) at 1073 K for 40 min with a heating rate of 10 °C/min. Samples ACOP2 and ACOP3 were prepared via carbonization at 1123 K for 1 h 30 min and 2 h, respectively, with a heating rate of 10 °C/min, followed by activation for 1 h 30 min and 1 h, respectively. In this way, products of different burn-off levels and therefore of different ash content, were produced. Carbon ACOP3ox was prepared by oxidation of ACOP3 using a saturated solution of $(NH_4)_2S_2O_8$ in 1 M H_2SO_4 in a carbon solution ration 1:10 at 298 K for 10 h, followed by washing with deionized water till no sulfates were detected in the filtrate. As it concerns olive pulp and olive stone they were immersed into a 10% H_2SO_4 solution for 6 h in a carbon solution ration 1:10 at 298 K and then washed with deionized water till neutral pH. The resulting materials were carbonized and activated as in the cases of ACOP and ACO to obtain ACOPWS and ACOWS carbons.

All samples were grounded and dried at 110 °C overnight before the determination of their chemical properties and the adsorption experiments.

2.2. Textural characterization

The samples were characterized by N_2 adsorption at 77 K performed with an Autosorb 1 N_2 porosimeter, by Hg porosimetry performed with a Quantachrom Autoscan 25 porosimeter as well as by their iodine number (mg iodine/g carbon). For this last determination 0.1 g of the sample was equilibrated for 1 h with a 0.1N standardized iodine solution. The remaining iodine was titrated with a 0.1N standardized sodium thiosulfate solution.

The ash content of all samples was obtained after burning a given amount of carbon in the presence of air at 973 K for 3 h and was calculated on a dry basis [14].

The pH of carbons was measured after suspending 1 g of the material in 20 ml CO_2-free distilled water for 48 h [14].

The point of zero charge, pH_{pzc}, of the activated carbons was obtained by following the reverse mass titration method [15] that is a modified version of the method proposed by Noh and Schwarz [16].

The samples were titrated with bases of different strength ($NaOCH_2CH_5$ in 100% ethanol, NaOH, $NaHCO_3$ and Na_2CO_3) following Bohem's method [17]. Since sodium ethoxide titrates carbonyl, carboxyl, lactones and phenolic groups, sodium hydroxide titrates carboxyl, lactone and phenolic, sodium carbonate titrates carboxyls and lactones and sodium bicarbonate titrates only carboxylic groups, one can obtain the number of the different acid groups. The bases, also present on the surface, were titrated with hydrochloric acid as has been described elsewhere [14].

2.3. Zinc adsorption experiments

Analytical grade hydrated zinc nitrate salts were used to prepare the stock solutions of the testing metal.

Adsorption experiments were performed without adding any buffer to control the pH. The final pH of zinc equilibrium solutions [$Zn(NO_3)_2$] for the adsorption isotherms and the

kinetic experiments varied within 6.0–7.0, with the exception of the pH of ACOP3ox adsorption isotherm solutions, which varied within 3.1–3.3. For carbons ACOP and ACOPox, the pH was adjusted with addition of HNO_3 and NaOH to pH 3 and 7, respectively, to evaluate the effect of different pH in the adsorption of zinc ions. Determination of metal ion concentration was performed by means of a Perkin-Elmer AAnalyst 100 atomic absorption spectrophotometer. Determination of nitrate ions at the final and initial solutions was measured by means of an ION85 ion analyzer of radiometer copenhagen.

2.3.1. Kinetic experiments

Rate of adsorption for specific cations was followed with time by using stoppered flasks containing 100 ml of aqueous solutions of $Zn(NO_3)_2{\cdot}6H_2O$ 1.9×10^{-4} M in which 25 g of carbon was added. In the case of ACOP sample two different concentrations of $Zn(NO_3)_2{\cdot}6H_2O$, 1.4×10^{-4} M and 8.6×10^{-4} M $Zn(NO_3)_2$, were used. The flasks were kept in a thermostat shaker bath at 298 K for various periods of time. Adsorption of activated carbons was followed with time at 15 and 30 min, 1, 2, 4, 6, 8, 16, 24, 48 and 72 h in different batches for each time interval.

2.3.2. Adsorption isotherms

Once the equilibrium time was known, the adsorption isotherms were determined for each sample. For this purpose, 0.25 g carbon and solutions ranging in between 0.31×10^4 and 9.8×10^{-4} M for Zn $(NO_3)_2{\cdot}6H_2O$, were shaken for 48 h at 298 K. In the case of samples originated from SEOP, the upper limit for Zn^{2+} adsorption isotherm was 2.94×10^{-3} M Zn $(NO_3)_2{\cdot}6H_2O$.

3. Results and discussion

3.1. Textural characterization

The N_2 adsorption isotherms at 77 K are demonstrated in Fig. 1. The ACOP, ACA, ACP isotherms correspond to type I of the IUPAC classification [17], exhibiting a knee at $P/P_0 < 0.01$, typical for relatively narrow micropores. The ACO, ACOP2 and ACOP3 isotherms correspond to type IV isotherm according to the IUPAC classification. They posses hysteresis loops between the adsorption and desorption branch, typical of type IV isotherms, indicating mesoporous materials. Shape of the loop is informative about the pore geometry [18]. In our case the loop indicates slit shaped capillaries with parallel walls, but cannot give us a clear pore size distribution. In addition a high degree of microporosity is observed (initial part of the isotherm and shape of adsorption branch) indicating that these materials have a high degree of microporosity along with the mesoporosity.

Table 1 shows some physicochemical characteristics of the carbons derived from N_2 and Hg porosimetry. The nitrogen BET surface area (Table 1) of the carbons was obtained by applying the well-known BET equation [19,20] to the N_2 adsorption isotherms (Fig. 1). The cross-sectional area, i.e. the area occupied by an adsorbate molecule in the completed monolayer for the N_2 molecule at 77 K was taken as 16.2 $Å^2$.

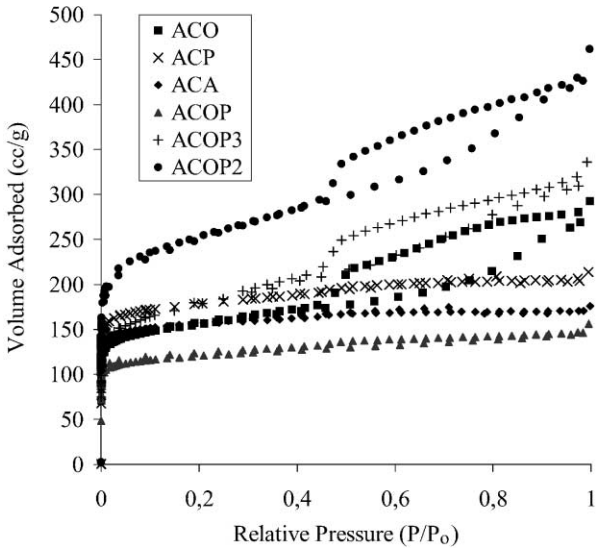

Fig. 1. Adsorption isotherms of N_2 at 77 K for activated carbons.

Additionally, adsorption isotherms were analyzed using the Dubinin–Radushkevich equation [21]:

$$\log W = \log(V_0 p) - k\left(\log \frac{P_0}{P}\right)^2 \tag{1}$$

where W the weight adsorbed at relative pressure P/P_0, V_0 the micropore volume, p the liquid adsorbate density and k a constant based on the pore size distribution shape.

A plot of $\log W$ versus $[\log P/P_0]$ gives a straight line with an intercept of $\log(V p)$ from which V_0, the micropore volume, can be calculated. DR surface areas and volumes are given in Table 1. In an attempt to further analyze the micropore structure of activated carbons, we have also applied the Dubinin–Astakhov method that is a generalized form of the DR method

Table 1
Physicochemical characteristics of activated carbons

Sample	S_{BET}	S_{DR}	Iodine number (mg iodine/g carbon)	Pore volume (cm^3/g)		
				V_{micro} (DR)	V_{meso}	V_{macro}
ACO	474	690	550	0.23	0.23	0.43
ACOWS	–	–	570	–	0.04	0.26
ACA	486	680	580	0.24	0.06	0.38
ACP	660	744	600	0.26	0.11	0.24
ACOP	364	508	478	0.18	0.07	0.55
ACOPWS	–	–	494	–	0.02	0.33
ACOP2	914	1012	910	0.36	0.37	0.83
ACOP3	646	670	640	0.24	0.31	0.58
ACOP3ox	–	–	270	–	0.09	0.52

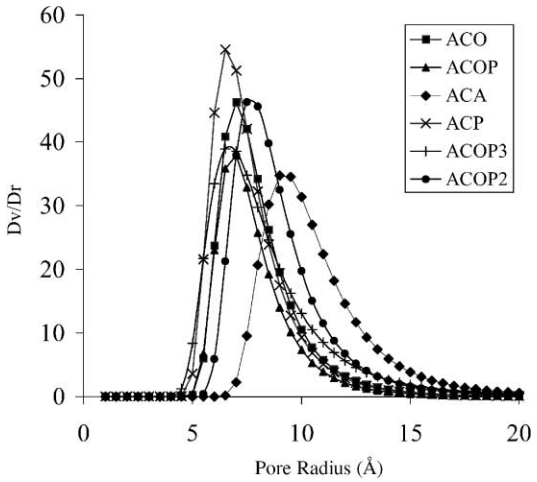

Fig. 2. DA plots for activated carbons.

and has been found to fit for adsorption data for heterogeneous micropores [22]. A plot of d(W/V)/dr versus results in the pore size distribution. D–A diagrams are given in Fig. 2.

We observe a clear shifting of ACOP3 towards higher pore radii if compared to the less activated ACOP carbon. ACA appears with wider micropores in the region of 7–18.5 Å while ACP carbon shows the higher micropore volume in the range of 5–10 Å pore radius.

Mesoporous volume was derived from mercury porosimetry (Fig. 3) for $dp > 40$ Å (V_1) and nitrogen porosimetry for 20 Å $< dp < 40$ Å (V_2 difference between the total

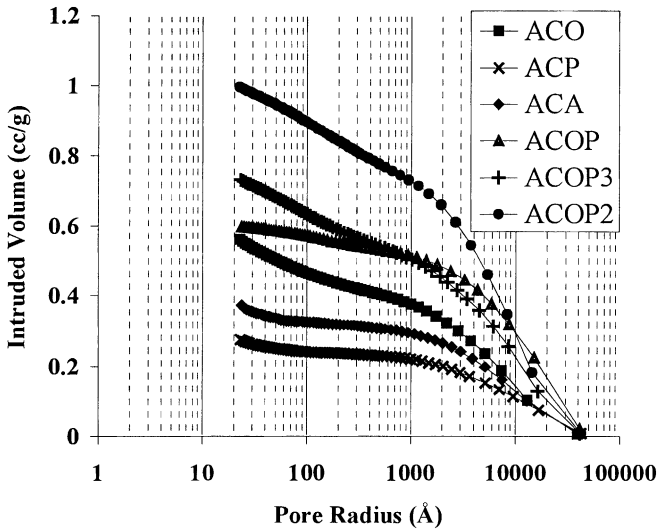

Fig. 3. Cumulative pore volumes for activated carbons.

and micropore volume for a given pore radius in the macroporous range and subsequent subtraction of the mercury porosimetry volume for the same pore radius). So as mesopore volume results as $V_{meso} = V_1 + V_2$.

Carbons of different origin prepared under the exact experimental conditions clearly show a variation in porosity development (Fig. 1, Table 1) attributed to the properties of the starting material. Olive stone (ACO carbon) favors mesoporosity while SEOP results in the higher macropore volume. Carbons ACOP2 and ACOP3 have been activated at higher burn-off than ACOP. Their porosity development follows the time of activation in terms of physicochemical characteristics. It is observed (Table 1) that ACOP2 has the higher volume in the whole pore range and the more developed surface area.

When the raw material was washed with sulfuric acid to remove the ash, the resulting ACOWS, ACOPWS carbons, comparing with ACO and ACOP, respectively, showed significantly lower gasification levels (Table 2) and a decrease in mesopore (more profound for ACOWS) and macropore volume (Table 1). Iodine number was not much affected showing that the removal of the inorganic matter has mainly influenced the larger pores. In this case, we observe that the higher ash content in the same raw material (Tables 1 and 2) accelerates the gasification process.

Oxidation of ACOP3 carbon lowered the iodine number, due to the presence of acidic groups, which block the pore entrances of micropores. The macroporosity did not show a significant change while mesoporosity above 40 Å pore diameter (Hg results) is also reduced up to 50%.

The ash content (Table 2) of SEOP activated carbons, increases during activation but the measured values (ash-m) are lower than the calculated ones (ash-c) based on the precursor composition and suggesting that the inorganic matrix is not affected. Hence we can conclude that the activation can affect not only the carbonaceous part but also the inorganic matter

Table 2
Ash content, burn-off and yield of activated carbons

Sample	Ash-m (%)	Ash-c[a] (%)	Burn-off (%)	Yield (%)
OP (SEOP)	1.8		–	–
$(OP_{H_2SO_4})$[b]	0.3		–	–
ACOP	6.5	8.0	18	22.6
ACOPWS	1.2		7	24.20
ACOP3	6.8	8.7	29	20.6
ACOP3ox	1.0		29	20.6
ACOP2	7.9	11.8	44	15.3
O (olive stone)	1.6		–	–
$(O_{H_2SO_4})$[b]	0.2		–	–
ACO	7.0	7.9	31.2	20.2
ACOWS	0.9		6	24.3
A (apricot)	0.3		–	–
ACA	1.8	1.3	12	23.8
P (peach)	0.4		–	–
ACP	0.6	1.6	11	24.9

[a] Ash-c = (ash of the precursor) × 100/yield.
[b] Precursors washed with H_2SO_4.

Table 3
pH and pH_{pzc} of activated carbons

Sample	pH	pH_{pzc}
ACO	10.5	10.2
ACOWS	6.5	6.6
ACA	10.3	9.9
ACP	10.0	9.8
ACOP	11.2	11.0
ACOPWS	6.1	6.3
ACOP3	10.9	10.8
ACOP3ox	2.7	3.1
ACOP2	10.7	10.5

of the samples. However, according to the ash content data (Table 2), the amount of the carbonaceous and inorganic part removed depends on the different precursors.

The pH of ACOP (Table 3) is higher among the carbons of different origin. Increase of activation time lowers the pH accordingly. The pH_{pzc} (Table 3) of carbons of different origin, prepared under the same experimental conditions is given in Fig. 4. On the basis of pH, all samples are of the H type being more basic with the exception of ACOP3ox carbon, which is of the L type being more acidic and of ACOWS and ACOPWS carbons, which are neutral.

Surface oxides of carbon products are given in Table 4. We observe that SEOP carbons have a significantly higher number of basic groups (reaction with HCl) if compared to the carbons derived from different starting materials prepared under the same experimental conditions and a higher number of sodium ethoxide titrable surface charges. Oxidation increases the total acidic groups (Table 4) on carbon surface lowering the pH (Table 3). Specific acidic groups for carbon ACOP3ox have been measured, with the above mentioned Boehm's method [15], as follows: [Carboxyls] = 1.00 meq./g, [Lactones] = 0.18 meq./g, [Phenols] = 0.73 meq./g. Treatment of the raw material with H_2SO_4 (removal of ash) lowers the total basicity of carbons ACOPWS and ACOWS whereas their total acidity remains unaltered. The number of carbonyl groups increases and this is more profound for carbon ACOWS than ACOPWS.

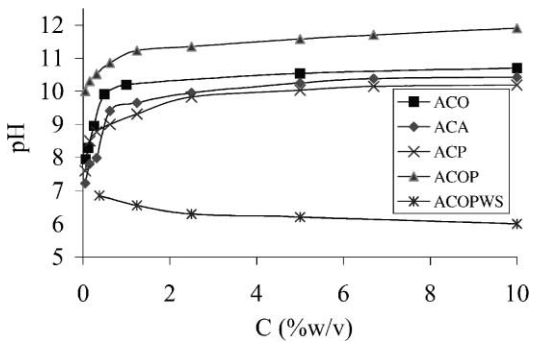

Fig. 4. pH_{pzc} for some activated carbons.

Table 4
Surface groups of activated carbons

Sample	Surface oxides (meq./g)		
	Carbonyls	NaOH	HCl
ACO	0.40	0.20	1.76
ACOWS	1.28	0.20	1.19
ACA	0.39	0.20	1.81
ACP	0.50	0.20	1.10
ACOP	0.73	0.29	2.72
ACOPWS	0.60	0.20	1.54
ACOP2	0.65	0.05	3.43
ACOP3	0.65	0.10	3.17
ACOP3ox	0.00	1.92	0.05

3.2. Zinc adsorption

The pH of all equilibrium solutions was below the pH where metal hydroxide chemical precipitation occurs, which has been estimated at pH > 8.4 (hydrolysis product at 25 °C) for the higher initial metal concentration. Under these conditions, metal removal from solution may be accomplished via interaction with the carbon surface.

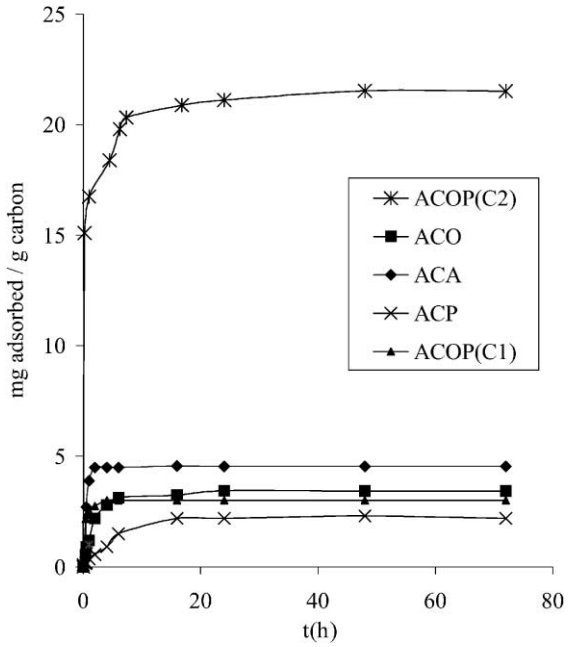

Fig. 5. Kinetic curves of Zn^{2+}: (a) 1.4×10^{-4} M; (b) 8.6×10^{-4} M for ACOP carbon and 1.9×10^{-4} M adsorption at 298 K for activated carbons of different origin.

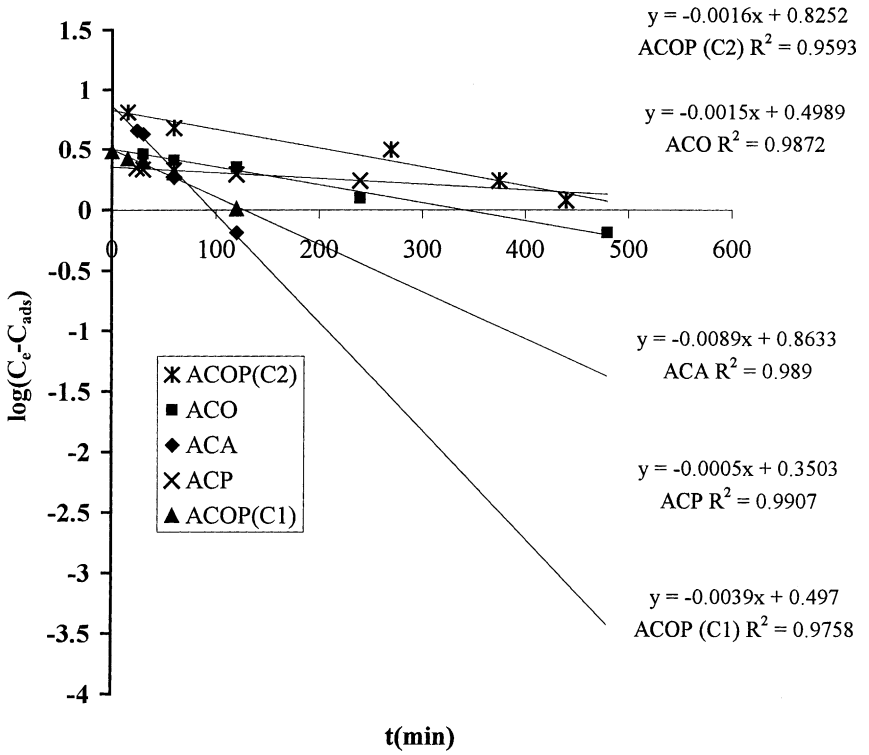

Fig. 6. Lagegren plots of Zn^{2+} adsorption for activated carbons of different origin.

Kinetic studies on metal adsorption of the activated carbons are shown in Fig. 5. Kinetic study on Zn^{2+} adsorption from ACOP carbon was performed in two concentrations due to the remarkably high rate of adsorption at the lower concentration. It was observed that the equilibrium is reached within 10 h for Zn^{2+}. Kinetic data were treated with the following form of Lagegren [23] equation (Fig. 6):

$$\log(q_e - q_{ads}) = \log q_e - \frac{K_{ads} t}{2.303} \tag{2}$$

where q_e and q_{ads} the amount of metal adsorbed at the equilibrium and at any time t and K_{ads} adsorption rate constant (Table 5). All the carbon/Zn^{2+} solution systems attain satisfactory fit to the model.

Additionally it was estimated the distribution coefficient k_d (Table 5) from the following equation:

$$k_d = \frac{rV}{100 - r} m \tag{3}$$

where k_d is the distribution coefficient, r percent removal, V volume of the solution, m weight of carbon used. This coefficient defines the selectivity of a carbon towards a specific molecule [24]. ACOP carbon shows significantly higher removal ability for Zn^{2+}, than

Table 5
Lagegren constants K_{ads} and distribution coefficients k_d for Zn^{2+} adsorption

Sample	K_{ads} (min^{-1})	r (%)	V/m (ml/g)	k_d
ACA	0.0012	44	400	314.29
ACP	0.0205	91	400	4044.44
ACO	0.0035	68.6	400	873.89
ACOP (C1)	0.0090	100	400	–
ACOP (C2)	0.0037	98	400	19600

the other carbons reaching almost 100% of the initial concentration, even in concentrated solutions [8.6×10^{-4} M $Zn(NO_3)_2$].

Once the equilibrium time was known adsorption isotherm studies for all four carbons at 48 h, were performed. The respective adsorption isotherms for Zn^{2+} are given in Fig. 7. The isotherms have been classified according to Giles' classification [25]. Giles has classified adsorption isotherms into four main groups: L, S, H and C. According to the above classification all carbons, with the exception of ACP and ACOP3ox, show H_2 isotherms. H_2 type explains the higher reactivity of these carbons towards Zn^{2+} ions. As more sites are filled, it becomes difficult for the solute molecules to find a site for adsorption so as the rate of adsorption decreases. ACP and ACOP3ox carbons follow an S_2 isotherm at unadjusted pH, having their active sites filled at low concentrations. Their saturation occurs at low levels of adsorption.

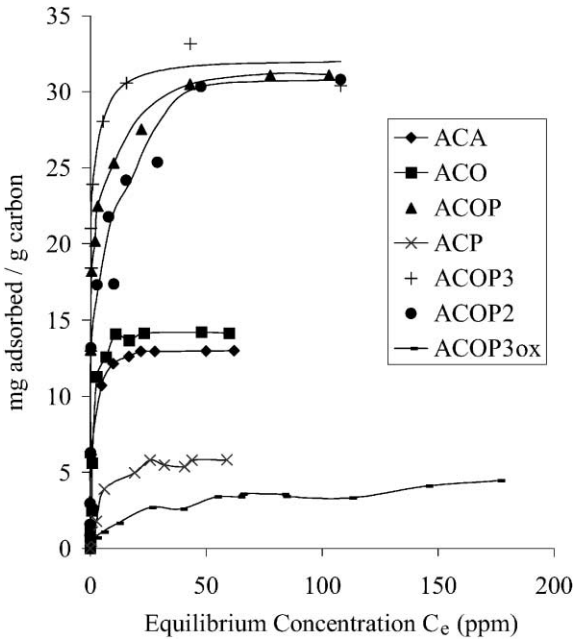

Fig. 7. Adsorption isotherms of Zn^{2+} at unjusted pH for activated carbons at 298 K.

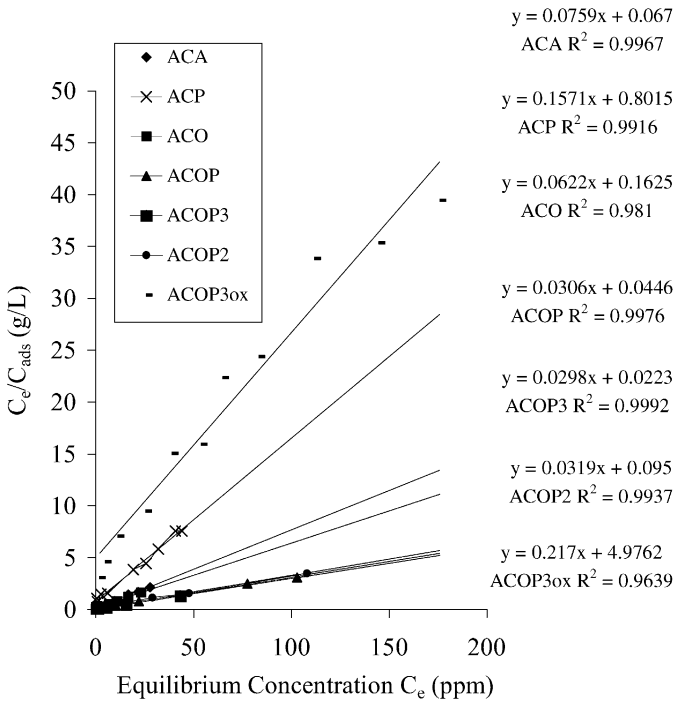

Fig. 8. Langmuir isotherms of Zn^{2+} adsorption at unjusted pH for activated carbons.

Data (Fig. 8) obtained from the adsorption isotherms were fitted to the linearized form of Langmuir [26]:

$$\frac{C_e}{C_{ads}} = \frac{1}{(k\,C_{max})} + \frac{C_e}{C_{max}} \tag{4}$$

where C_{ads} the amount adsorbed, C_e the adsorbate equilibrium concentration, k and n isotherm constants (k differs for each model) and C_{max} the maximum amount adsorbed (Table 6).

Table 6
Physicochemical parameters of Zn^{2+} adsorption for activated carbons at unjusted pH

Activated carbon	k (l/mg)	C_{max} (mg/g)	$-\Delta G^o$
ACA	1.130	13.175	27.78
ACP	0.196	6.370	23.44
ACO	0.380	16.08	25.10
ACOP	0.686	32.68	26.54
ACOP3	1.340	33.56	28.20
ACOP2	0.336	31.35	24.74
ACOP3ox	0.044	4.61	19.73

Standard Gibbs free energy ΔG^{o} for the adsorption process (Table 5) has been calculated for each system, from the following equation:

$$\Delta G^{o} = -RT \ln k \tag{5}$$

where R the ideal gas constant (8.31433 J/mol K), T temperature (K) and k Langmuir constant.

Despite the difference in surface area, and pore volume (micro to macropores), carbons ACOP2 and ACOP3, possessing similar amounts of surface groups (Table 4), show similar adsorption levels for zinc ion. Additionally, ACOP carbon although has a remarkably less developed surface area and porosity (Table 1) and a slightly lower number of basic surface groups (Table 4), if compared to the aforementioned carbons, adsorbs similar amounts of the test metal. It is also observed that all the untreated carbons from SEOP have large macroporous volume ($\geq 0.55\ cm^3/g$).

The oxidized ACOP3ox carbon having lower iodine number and mesopore volume and negligible ash content, compared to ACOP3, presents lower adsorption maxima, at unadjusted pH. The former possesses 50% carboxylic groups (strong acidity) and 38% phenols (weak acidity). Carbons ACO and ACA, prepared under the same experimental conditions, appear with similar pH and amount of both acidic and basic surface groups (Table 4), reaching similar levels of adsorption, although they have different degree of inorganic matter. Carbon ACP, possessing the lowest amount of basic surface groups, appears with the lowest adsorption, if compared to carbons ACOP, ACA and ACO.

With reference to the speciation diagram of aqueous zinc solution [27], it can be seen that under both the initial and the equilibrium solution's pH, the predominant species is always Zn^{2+}.

The results of surface groups determinations (Table 4) clearly indicate that the steam activation at 800 °C increases the basic surface groups of the SEOP samples, with increasing activation time. It has been reported [2,15] that the basic surface properties arise from two types of interactions: (1) electron-donor acceptor (EDA) complex formation that predominates in carbons of low oxygen content and (2) pyrone-type groups contribution, which prevails in carbons of high oxygen content.

Based on a constructed curve by Lopez-Ramon et al. [28] showing the correlation between pH_{pzc} and oxygen content [O], the untreated SEOP carbons studied in this current work are of low oxygen content, less than 0.8 mmol [O]/g. We can conclude, that the basicity of these carbons arise from their ability to form EDA complex. Hence, the mechanism of adsorption on the basic carbons studied is mainly due to the EDA complexation of the delocalised (absence of electron-withdrawing oxygen functional groups) π-electrons of the carbon crystallites basal planes and ion zinc species. It is seemed that these carbons can adsorb cations from solutions with enough strength to render the surface positively charged. However, the exact nature of the oxygen-free Lewis basic sites remains unclear.

Furthermore, adjustment of solution pH at 3, for carbon ACOP, resulted in a lower adsorption (Fig. 9) than when adsorption was performed at pH $\sim$ 6.8. At low pH values there is a competition between H^+ and Zn^{2+} ion species for the sites of adsorption, due to the high H^+ concentration, while at higher pH this effect is diminished. Seco et al. [29] and Carrott et al. [30] show that the pH range, where maximum adsorption occurs, lies within pH 5–7, confirming our observation for low adsorption at pH 3.

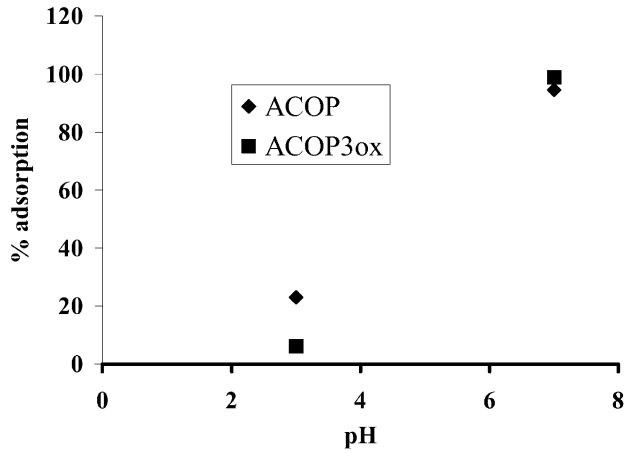

Fig. 9. Effect of pH on zinc adsorption for the oxidized and the non-oxidized carbons.

The adsorption of Zn^{2+} by ACOPWS and ACOWS carbons was kept at low levels (Fig. 10). Treatment of the precursors SEOP and O with H_2SO_4 decreased the pH_{pzc} of the resulting carbons (Table 3) and subsequently increased their surface oxygen content. Their basicity might arise both from EDA complex and the contribution of pyrone-type groups. The later may do not participate in the adsorption of cations.

The effect of the presence of nitrate ions has been also investigated (Fig. 11). Since the pH of all solutions is lower than the pH of the carbons (with the exception of ACOP3ox),

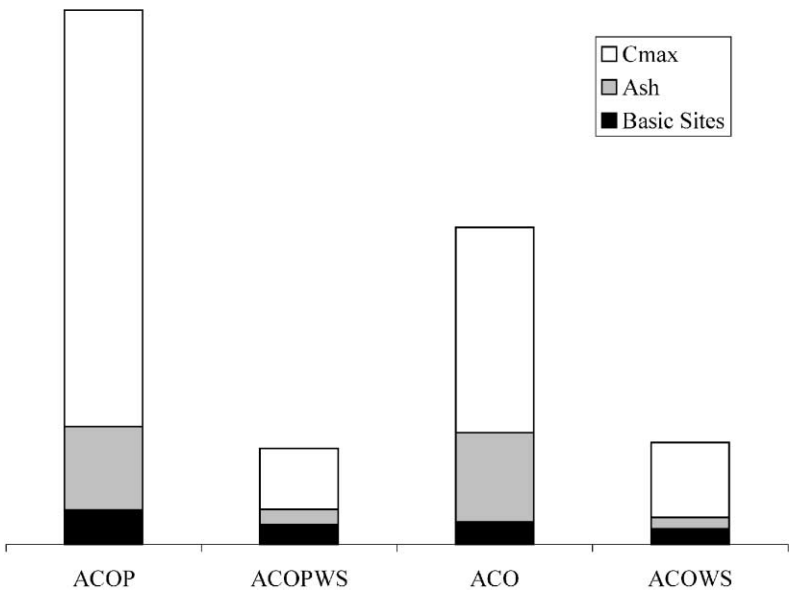

Fig. 10. Effect of basic groups and ash on zinc adsorption.

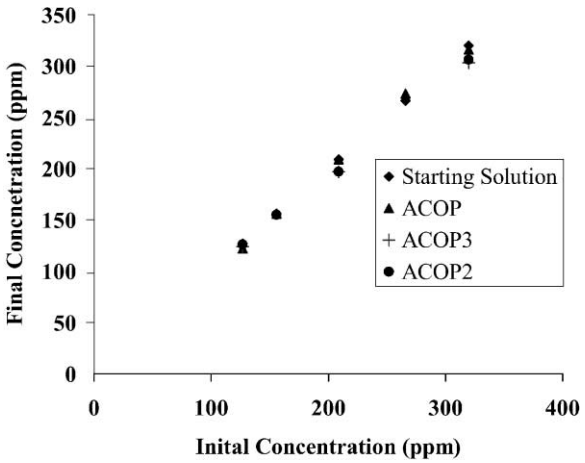

Fig. 11. Nitrate concentration in aq. zinc solutions.

the adsorbents are considered as positively charged so as if ion exchange was the main adsorption mechanism on carbon surface, the nitrate anions would significantly decrease within the solution. However, no nitrate adsorption was observed indicating that the adsorption of metal ions occurs directly on carbon surface without anions to be involved. The most adequate explanation, for the behavior of nitrate ions, arises from the requirement for electroneutrality. Thus, counterions, such as OH^- or $NO_3{}^-$ would be held loosely in the diffuse part of a secondary "double layer", the inner part of which would result in a positively charged carbon surface being neutralized in solution by a cloud of more or less mobile and exchangeable anions. $NO_3{}^-$ ions compared to OH^- ions are larger and they travel slower within the solution.

When adsorption, for carbon ACOP3ox, was performed at pH $\sim$ 3 (physical pH) the removal was kept at low levels. This is attributed to the fact that acidic groups are not deprotonated at this pH (lactones $pK_a = 7$–9, phenols $pK_a = 8$–11) while there is only a small fraction of strong acidic groups (carboxyl $pK_a = 3$–6) deprotonated. Furthermore, the presence of acidic groups in the oxidized ACOP3ox carbon, cause localization of the π-electrons of the basal planes, so as there is no significant interaction between the latter and the metal ion species. On the contrary, at pH $= 7$ (Fig. 9), although the localization still exists, dissociation of acidic groups, especially carboxylic groups and in a lower degree of lactones and phenols, leads to an ion exchange adsorption on carbon surface.

4. Conclusions

The results obtained show that activated carbons prepared from SEOP, an inexpensive precursor of the kernel-oil processing, can be readily used for the removal of aqueous zinc species.

Steam activation at 800 °C leads to H-type carbons.

Comparison of SEOP carbon with carbons of different origin but prepared under the same experimental conditions shows that the former has the highest adsorption capacity. The adsorption of zinc by these carbons, is favored at a pH range ∼5.5–7. For SEOP carbons, we observe high pH_{pzc} values, indication of low oxygen content, and a significant number of basic groups, along with an efficient macroporous volume. All these factors result in higher adsorption levels, despite the fact that the carbons are positively charged. In this case adsorption seems to be mainly governed by the dispersion forces between the cations and the delocalised π-electron system of the graphene layers.

Oxidation of SEOP carbon with $(NH_4)_2S_2O_8$ resulted in a carbon with greater zinc uptake than observed for the non-oxidized one at the pH range 5.5–7. In this case, zinc uptake appears to be correlated with the total acidic surface oxygen groups, i.e. carboxyls, phenols and lactones. In the pH range 5.5–7 the oxidized carbon is negatively charged (adsorption pH $>$ carbon's pH) and has a clear tendency to adsorb positively charged species by electrostatic forces, i.e. ion exchange due to the deprotonation of carboxyls and a fraction of lactones and phenols. The presence of electron-withdrawing oxygen functional groups reduces its dispersive adsorption potential by decreasing the π-electron density in the graphene layers, since it causes localization of the electrons in the neighborhood of the surface oxides.

Steam activation of the treated, with H_2SO_4, precursors yields activated carbons (ACOPWS, ACOWS) with lower surface basicity, higher oxygen content and much lower zinc uptake.

The results confirm that the liquid-phase adsorption on carbons is governed either by electrostatic attraction (ACOP3ox) or by dispersion forces (ACOP, ACOP2, ACOP3).

In the case of adsorption of inorganic compounds from aqueous solutions, the chemical nature of the adsorbent, determined by the amount and nature of the surface groups has, in general, more influence than its surface area and porosity.

Acknowledgements

This work was supported by NAGREF (project Dimitra no. "D" 95 VI/4).

References

[1] S. Yiakoumi, J. Chen, in: A. Dabrowski (Ed.), Adsorption and its Applications in Industry and Environmental Protection, Vol. 120, Elsevier, Amsterdam, 1998, p. 285.
[2] L.R. Radovic, Chemistry and Physics of Carbon, Vol. 27, Marcel Dekker, New York, 2001.
[3] H. Jankowska, A. Swiatkowski, J. Choma, Activated Carbon, WNT, Warsaw, 1985.
[4] R. Dobrowski, M. Jaroniec, M. Kosmulski, Carbon 24 (1986) 15.
[5] R.C. Bansal, J.B. Donnet, F. Stoeckli, Active Carbon, Marcel Dekker, New York, 1988.
[6] A. Capelle, F. De Vooys, in: N.V. Norit (Ed.), Activated Carbon a Fascinating Material, Amersfoot, The Netherlands, 1983.
[7] H. von Kienle, E. Bader, Aktivkohle und ihre industrielle Anwendung, Ferdinand Enke Verlag, Stuttgart, 1980.
[8] M. Smisek, S. Cerny, Active Carbon, Elsevier, New York, 1970.
[9] P. Galiatsatou, Ph.D. Thesis, NTUA, Athens, 1994.

[10] M.A. Ferro-Garcia, J. Rivera-Utrilla, J. Rodriguez-Gordillo, I. Bautista-Toledo, Carbon 26 (1988) 363.
[11] C.A. Leon, Y. Leon, J.M. Solar, V. Kcalemma, L.R. Radovic, Carbon 30 (1992) 797.
[12] S. Karabult, A. Karabakan, A. Denizli, Y. Yurum, Sep. Purif. Technol. 18 (2000) 177.
[13] W. Shaobin, G.Q. Max Lu, Carbon 36 (3) (1998) 283.
[14] J. Rivera-Utrilla, M.A. Ferro-Garcia, Ads. Sci. Techn. 3 (1986) 293.
[15] K. Gergova, N. Petrov, L. Butuzova, V. Minkova, L. Isaeva, J. Chem. Tech. Biotechnol. 58 (1993) 321.
[16] J.S. Noh, J.A. Schwarz, J. Colloidal Int. Sci. 130 (1989) 137.
[17] H.P. Boehm, in: H. Eley Pines, P.R. Weisz (Eds.), Advances in Catalysis, Vol. 16, Academic Press, New York, 1966.
[18] S. Brunauer, L.S. Deming, W.E. Deming, E.J. Teller, J. Am. Chem. Soc. 62 (1940) 1723.
[19] R.M. Barrer, J.W. Sutherland, Proc. Roy. Soc. 439 (1956) A237.
[20] S. Brunauer, H. Emmett, E. Teller, J. Am. Chem. Soc. 60 (1938) 309.
[21] M.M. Dubinin, L.V. Radushkevich, Proc. Acad. Sci. U.S.S.R. 55 (1947) 331.
[22] M.M. Dubinin, V.A. Astakhow, Adv. Chem. 102 (1971) 69.
[23] C. Namasivayam, K. Cadiverlu, Chemosphere 34 (1977) 377.
[24] L.L. Ames, Am. Mineral 47 (1962).
[25] C.H. Giles, D.A. Smith, J. Colloidal Int. Sci. 47 (1974) 3.
[26] I. Langmuir, J. Am. Chem. Soc. 40 (1918) 1361.
[27] J.N. Butler, Ionic Equillibrium, A Mathematical Approach, Addison-Welsey, Reading, MA, 1964.
[28] M.V. Lopez-Ramon, F. Stoeckli, C. Moreno-Castilla, F. Carrasco-Marin, Carbon 37 (1999) 1215.
[29] A. Seco, P. Marzal, C. Gabaldon, J. Chem. Tech. Biotechnal. 68 (1997) 23.
[30] P.J.M. Carrott, M.M.L. Ribeiro Carrott, J.M.V. Nabais, J.P. Ramahldo Prates, Carbon 35 (1997) 403.